F. DĄBROWSKI[©1*], Ł. CIUPIŃSKI[©1], J. ZDUNEK[©1], W. CHROMIŃSKI[©1],
M. KRUSZEWSKI[©1], R. ZYBAŁA[©1,2], A. MICHALSKI[1], K.J. KURZYDŁOWSKI[©1]

MICROSTRUCTURE AND THERMOELECTRIC PROPERTIES OF DOPED FeSi₂
WITH ADDITION OF B₄C NANOPARTICLES

β-FeSi$_2$ with the addition of B$_4$C nanoparticles was manufactured by sintering mechanically alloyed Fe and Si powders with Mn, Co, Al, P as p and n-type dopants. The consolidated samples were subsequently annealed at 1123 K for 36 ks. XRD analysis of sinters after annealing confirmed nearly full transformation from α and ε into thermoelectric β-FeSi$_2$ phase. SEM observations of samples surface were compliant with the diffraction curves. TEM observations allowed to depict evenly distributed B$_4$C nanoparticles thorough material, with no visible aggregates and establish grain size parameter $d_2 < 500$ nm. All dopants contributed to lower thermal conductivity and Seebeck coefficient, with Co having strongest influence on increasing electrical conductivity in relation to reference FeSi$_2$. Combination of the addition of Co as dopant and B$_4$C nanoparticles as phonon scatterer resulted in dimensionless figure of merit ZT reaching 7.6×10^{-2} at 773 K for Fe$_{0.97}$Co$_{0.03}$Si$_2$ compound.

Comparison of the thermoelectric properties of examined sinters to the previously manufactured of the same stoichiometry but without B$_4$C nanoparticles revealed theirs overall negative influence.

Keywords: iron disilicide, nanoparticles, thermoelectrics

1. Introduction

Possibility of using thermoelectric generators (TEGs) to exploit waste heat makes the thermoelectric materials - exhibiting a significant Seebeck effect, to revive with the development of novel manufacturing methods, allowing to reach challenging goal of enhancing *ZT* - a dimensionless figure of merit describing material thermoelectric effectiveness [1]. With the thermoelectric materials efficiency increasing, nowadays TEGs find more and more applications. One of the well known thermoelectric material, initially documented in 1960s [2] is iron disilicide (β-FeSi$_2$). It is a semiconductor with a band gap of 0.85 eV at room temperature, characterized by a high Seebeck coefficient, superior oxidation resistance and high working temperature range (up to 1200 K) [3-5].

With its non-toxicity and availability of the substrates used to fabricate β-FeSi$_2$, this compound draws much attention in the context of TEGs applications. The thermoelectric properties of β-FeSi$_2$ are quite low comparing to novel thermoelectric material such as for example scutterudites [6]. With many manufacturing methods already explored, still there have not been proven manufacturing method of FeSi$_2$ efficient in terms of reducing production cost and resulting in high performance material.

The goal of this work is to investigate the influence of addition of B$_4$C nanoparticles on thermoelectric properties of p and n-type doped β-FeSi$_2$ manufactured using mechanical alloying (MA) and pulse plasma sintering [7].

The selection of B$_4$C nanoparticles as an extra addition was motivated for following reasons: a) B$_4$C itself is a good thermoelectric material [8], b) addition of B$_4$C particles to other thermoelectric materials resulted in enhanced properties [9].

The manufacturing method combination was chosen as previous results indicate that PPS offers unique combination of rapid heating/cooling and short processing time, essential for preserving nanometer size of the consolidated powders [10,11]. It was successfully used to manufacture wide range of materials [12,13] including ceramics [14]. Retaining fine-grained structure is an important challenge in the case of the materials for thermoelectric applications as increasing share in volume of grain boundaries is one of efficient ways to reduce thermal conductivity [15]. Finally, authors previous study [16] confirmed

[1] WARSAW UNIVERSITY OF TECHNOLOGY, FACULTY OF MATERIALS SCIENCE AND ENGINEERING, 141 WOŁOSKA STR., 02-507 WARSZAWA, POLAND
[2] ŁUKASIEWICZ RESEARCH NETWORK, INSTITUTE OF MICROELECTRONICS AND PHOTONICS, 32/46, LOTNIKÓW STR., 02-668 WARSZAWA, POLAND

* Corresponding author: franekandroid@gmail.com

1158

that such manufacturing route yields promising results in terms of enhancing thermoelectric properties of β-FeSi$_2$.

In order to assess the influence of addition of B$_4$C nanoparticles to p and n-type doped β-FeSi$_2$ on its thermoelectric properties, a series of specimens have been prepared using MA and PPS of n (Co, P) and p (Mn, Al) type doped β-FeSi$_2$ with the 1% (by weight) of B$_4$C. The amount of B$_4$C was selected based on previous report – [17], where the authors indicated that among of 1, 2, 4 and 6 wt. % addition of dispersed microparticles of B$_4$C into β-FeSi$_2$ the 1% content resulted in the highest figure of merit in bulk material.

The obtained samples were characterized in terms of their structure and properties, including the thermoelectric power and compared with samples without B$_4$C nanoparticles addition, manufactured using the same route and identical stoichiometry.

2. Experimental procedure

Elemental powders of Fe (purity 99.99% –200 mesh, American Elements), Si (purity 99.999% –325 mesh, Alfa Aesar), Co (purity 99.5% –325 mesh, Electronic Space Products International), Mn (purity 99.95% –325 mesh, Alfa Aesar), Al (purity 99.95% –100,+325 mesh, Sigma-Aldrich) and Fe$_2$P (purity 99.5% –40 mesh, Sigma-Aldrich), B$_4$C (99+, nano powder 45-55 nm, US Research Nanomaterials INC.) were used to prepare n and p-type FeSi$_2$ powders using MA method. In Table 1, 4 selected compounds are shown. Each dopant and its amount resulting in highest thermoelectric power was chosen based on literature review (Mn [18-21], Co [5,20,22-24], Al [19,25-26], P [27]) and former experience of the authors.

TABLE 1

Synthesized compounds with the addition of B$_4$C nanoparticles

Dopant	Mn	Co	Al	P
Compound	Fe$_{0.92}$Mn$_{0.08}$Si$_2$	Fe$_{0.97}$Co$_{0.03}$Si$_2$	FeSi$_{1.93}$Al$_{0.07}$	FeSi$_{1.95}$P$_{0.05}$

Compounds were mechanically alloyed in Retsch planetary ball mill PM 100 in argon atmosphere. The mixtures of substrates without B$_4$C nanoparticles were sealed in 500 ml steel containers with 50 balls, inside glove box in argon atmosphere. The mixture-to-ball weight ratio was 1:10 for all samples. Sealed samples were subjected to milling. B$_4$C nanopowder was added to the mechanically alloyed compounds to evenly distribute particles within prepared powder. The milling procedure parameters are shown in Table 2.

The mechanically alloyed compounds were PPS sintered in graphite dies with the diameter of 10 mm. The samples were sintered to an observable shrinkage stop (punch travel) at 1373 K and held for 30 s at a pressure of 50 MPa. The current pulse stabilizing the temperature occurred every 0.4-0.6 s. The time between pulses during sintering was adjusted live for the process to maintain the same sintering temperature for all samples. An-

TABLE 2

Milling parameters of doped FeSi$_2$ with the addition of B$_4$C nanoparticles

Type	Mode	Effective milling period	Break	Interval	Rotation speed
Preliminary	Alternating	2 min	0	1 min	100 rpm
Main	Alternating	40 h	15 min	15 min	300 rpm
Addition of B$_4$C nanoparticles					
Preliminary	Alternating	2 min	0	1 min	100 rpm
Main	Alternating	10 h	15 min	15 min	300 rpm

nealing of bulk samples was conducted in vacuum, using sealed quartz tubes, at 1123 K for 36 ks.

The density, ρ, of the samples subjected to post sintering annealing was measured using the Archimedes method. Phase analyses were performed by X-ray diffraction (XRD, Bruker, D8 Advance, Cu K$_\alpha$). The XRD spectra were obtained in the 2Θ range of 15-60° where most characteristic peaks of Fe-Si system are located. Microstructure of powders and sintered samples were evaluated using scanning electron microscopy (SEM, Hitachi, SU-70) and the chemical composition of sinters with energy-dispersive spectroscopy (EDS). In order to observe the distribution of nanoparticles and the grain boundaries, a JEOL JEM 1200 EX transmission electron microscope was used. Images were taken using voltage of 120 kV in bright field (BF) and dark field (HAADF) modes. The Seebeck coefficient, S, as well as the electrical conductivity, σ, were measured using the standard four-probe method, in vacuum. The thermal diffusivity, D, was measured by the laser flash method (LFA, Netzsch, 457 MicroFlash) using samples with diameter of 10 mm and height of ~1 mm. The thermal conductivity, κ, was calculated according to the formula $\kappa = D\,C_p\rho$, where C_p – specific heat and ρ – density [27]. All measurements of S, σ, κ, were performed within the temperature range from 323 to 773 K.

3. Results and discussion

The relative densities of the sintered samples after the post-sintering annealing have been calculated under the assumption of the theoretical density of 4.93 g/cm^3 for un-doped iron silicide, taking into account true compositions of the doped samples and atomic mass differences between Fe, Si and dopants. The obtained values are listed in Table 3.

TABLE 3

The results of relative density measurements

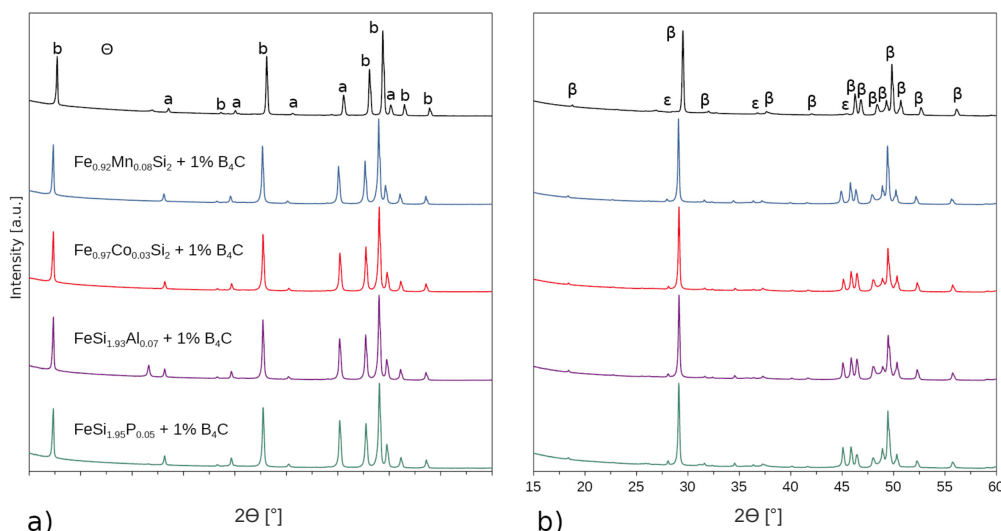| Sample	Relative density [%]
FeSi$_2$	94.93
Fe$_{0.92}$Mn$_{0.08}$Si$_2$ + B$_4$C	94.12
Fe$_{0.97}$Co$_{0.03}$Si$_2$ + B$_4$C	94.32
FeAl$_{0.07}$Si$_{1.93}$ + B$_4$C	95.74
FeP$_{0.05}$Si$_{1.95}$ + B$_4$C	93.91

Fig. 1. The XRD patterns for the samples: before (a) and after (b) annealing at 1123 K for 36 ks

The relative density was observed to be in the range of ~93-96%. Most of the samples are characterized by a satisfactory relative density above 94%. Obtained values are of the same range that the values obtained by other for materials produced by the SPS method [21,28]. Therefore, it should be concluded that the consolidation technique used in the study, pulse plasma sintering, and specified sintering parameters resulted in the desired, high density bulk material likewise observed for other PM consolidation techniques such as HP or SPS.

The XRD patterns shown in the Fig. 1 present that all samples with the addition of B_4C nanoparticles after annealing contain increased content of the residual ε phase, compared to the reference material – peak: $2\Theta = 45.125° – [210]$. This result should be attributed to hindered diffusion during the $\alpha + \varepsilon \rightarrow \beta$ phase reaction, caused by the presence of dispersed B_4C nanoparticles. XRD measurements demonstrated that the overall content of residual ε phase in samples with the addition of B_4C nanoparticles after annealing, is not negligible which might be sufficient in terms of negative influence of ε phase on thermoelectric properties. Maintaining lowest temperature and shortest annealing time, that is required to prevent excessive grain growth is a challenge in terms of obtaining β phase. Developed in previous study annealing parameters 1123 K for 36 ks proved to be sufficient. The same parameters used in this study turned out to be less accurate for samples with B_4C addition.

Fig. 2 shows the surfaces of doped samples with the addition of B_4C nanoparticles. A significant amount of residual ε phase was observed in the material after annealing. This observation is consistent with the X-ray structural analysis and indicates slowing down of the phase transformation $\alpha + \varepsilon \rightarrow \beta$ due to the presence of nanoparticles, which suppress Fe and Si atoms diffusion between the α phase and the ε phase.

In the Fig. 3, images of the structure of the material with the addition of nanoparticles, were shown. Characteristic black *dots* can be observed, corresponding to nanoparticles with a size from a few to several nm. The nanoparticles are evenly distributed throughout the entire volume of the material, including the

grain boundaries. The observed dispersion of nanoparticles in the manufactured material is satisfactory in terms of their influence on thermal conductivity [29]. Captured images allowed to outline distinctive grain boundaries and with the use of dedicated software [30], calculate grain size parameters (Table 4).

TABLE 4

Grain size

Parameter	Material
	$Fe_{0.97}Co_{0.03}Si_2$ + 1% B_4C
A [μm²]	0.19
d_2 [nm]	427

Calculated submicron values, significantly smaller comparing to other reported in literature: 1-10 [31], 1-100 [21], ~1 [28] μm, look promising in terms of enhancing thermoelectric properties as reducing grain size implicates reducing thermal conductivity [24]. Within some of the grains (see Fig. 3b) characteristic for β-phase order domains – lamellae-like structures [32] were observed, which emerged during manufacturing process.

Fig. 4 exhibits measurements of thermal conductivity, electrical conductivity, Seebeck coefficient and dimensionless figure of merit. κ is similarly lowered by the addition of Mn, Al or P with the strongest influence of Co as dopant. Comparing to the compounds without B_4C addition manufactured alike [16], the presence of dispersed nanoparticles stabilized thermal conductivity in the temperature range of the measurement – lowering κ for $FeSi_2$ with p-type dopants and increasing for n-type dopants, leaving $Fe_{0.97}Co_{0.03}Si_2$ with the lowest κ within the whole temperature range. Presence of B_4C nanoparticles lowered the increase of σ with the influence of dopants and observed metallic ε phase. The most significant factor in formula on $ZT – S$ was lowered for all samples in comparison to reference material and compounds without B_4C nanoparticles. All of the observed results implicate lower ZT than in identical compounds but without B_4C nanoparticles (Fig. 4.d). The highest value reached by $Fe_{0.97}Co_{0.03}Si_2$ with B_4C nanoparticles – 7.6×10^{-2} is nearly
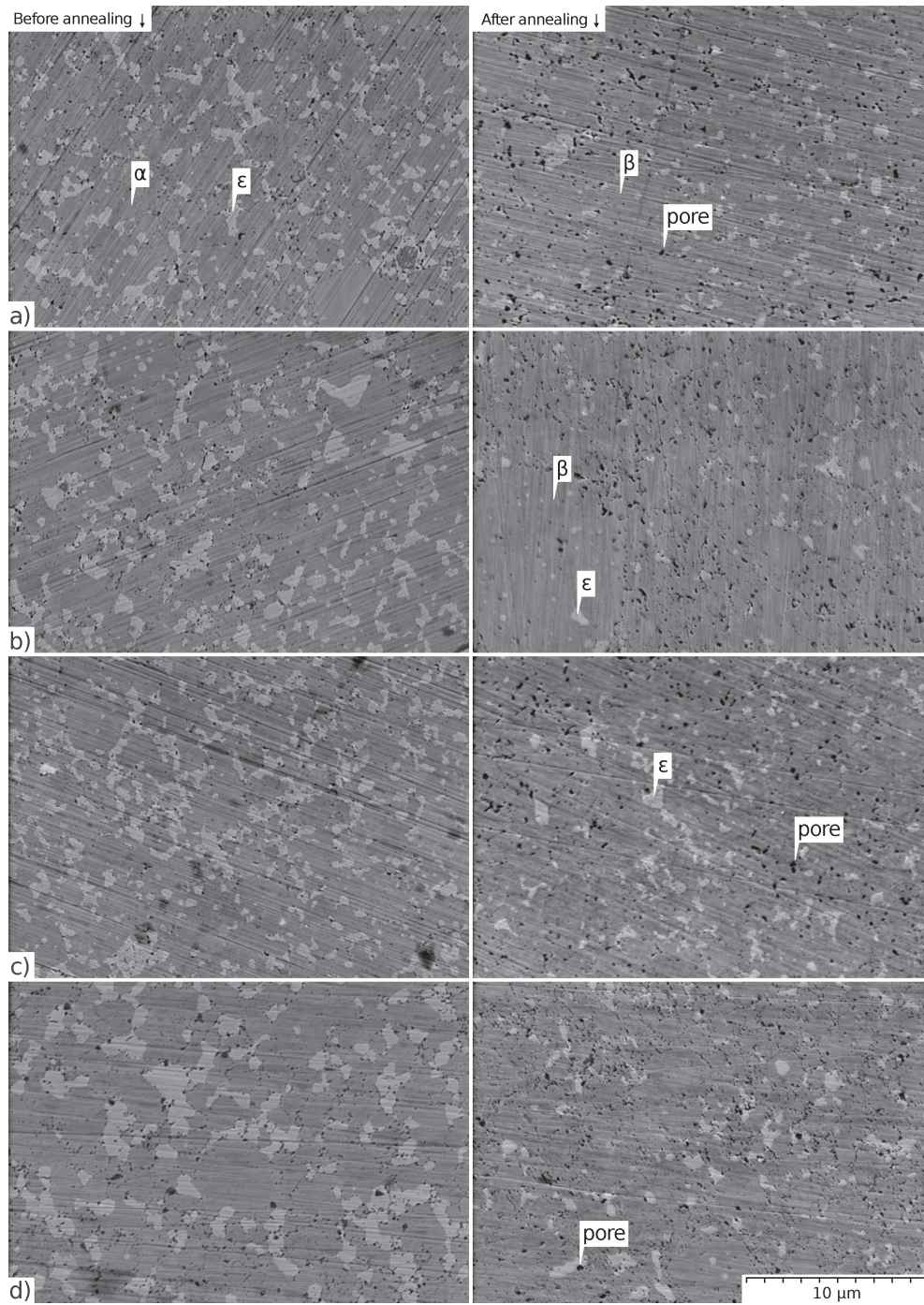
1160

Fig. 2. SEM images of the samples before and after post sintering annealing: a) $Fe_{0,92}Mn_{0,08}Si_2 + B_4C$; b) $Fe_{0,97}Co_{0,03}Si_2 + B_4C$; c) $FeAl_{0,07}Si_{1,93} + B_4C$; d) $FeP_{0,05}Si_{1,95} + B_4C$
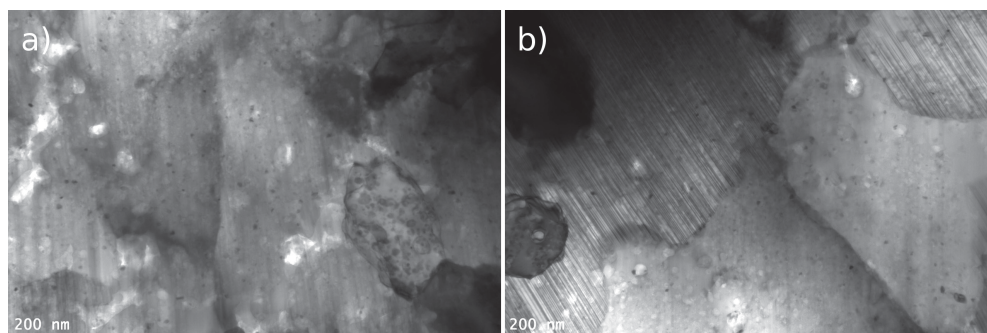

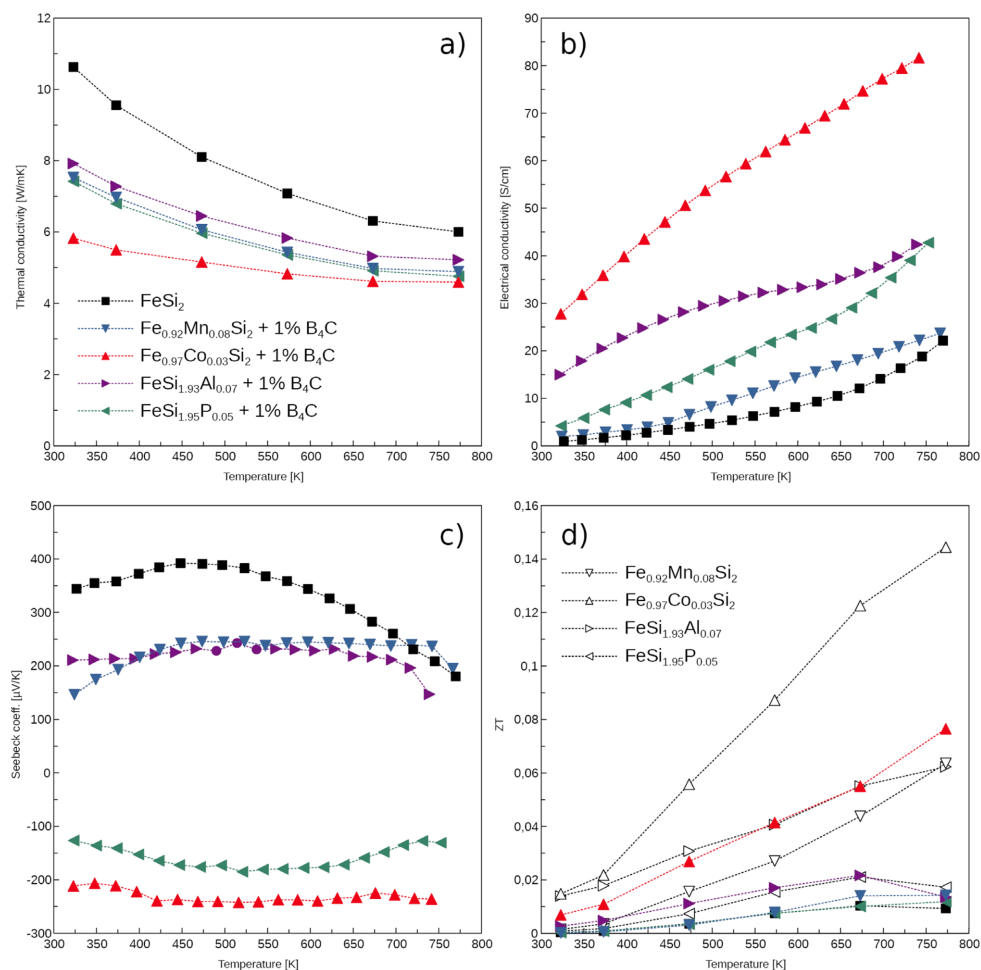Fig. 3. TEM images in bright field of a Co doped sample with B_4C nanoparticles

Fig. 4. Thermoelectric properties: a) Thermal conductivity; b) Electrical conductivity; c) Seebeck coefficient; d) Figure of merit *ZT*

half of 15×10^{-2} at 773 K for the initial $Fe_{0.97}Co_{0.03}Si_2$. As for the other dopants the negative impact is even higher.

It is not unambiguous that it is the sole influence of just the presence of B_4C nanoparticles as higher share of residual ε phase was observed for all sinters in relation to initial compounds in previous study. Thus further studies will be undertaken to clarify that.

4. Conclusions

Proposed manufacturing method allowed to produce doped iron disilicide with the addition of B_4C nanoparticles of satisfactory density and β phase content, with regular dispersion of nanoparticles in volume and submicron grain size. The sole addition of B_4C did not improve the thermoelectric properties of the $FeSi_2$ and slowed down the transformation of α and ε phases into the thermoelectric $β$-$FeSi_2$, which might contributed to the lower than expected thermoelectric properties of the doped sinters.

REFERENCES

[1] S. Twaha, J. Zhu, Y. Yan, B. Li, A comprehensive review of thermoelectric technology: Materials, applications, modelling and performance improvement, Renewable and Sustainable Energy Reviews **65**, 698-726 (2016).
DOI: https://doi.org/10.1016/j.rser.2016.07.034

[2] R.M. Ware, D.J. McNeill, Iron disilicide as a thermoelectric generator material, Proc. Inst. Electr. Eng. **111**, 178 (1964).
DOI: https://doi.org/10.1049/piee.1964.0029

[3] T. Kojima, Semiconducting and Thermoelectric Properties of Sintered Iron Disilicide, Phys. Stat. Sol. (A) **111**, 233-242 (1989).
DOI: https://doi.org/10.1002/pssa.2211110124

[4] M. Takeda, M. Kuramitsu, M. Yoshio, Anisotropic Seebeck coefficient in $β$-$FeSi_2$ single crystal, Thin Solid Films **461**, 179-181 (2004). DOI: https://doi.org/10.1016/j.tsf.2004.02.066

1162

[5] M. Ito, T. Tada, S. Katsuyama, Thermoelectric properties of $Fe_{0.98}Co_{0.02}Si_2$ with ZrO_2 and rare-earth oxide dispersion by mechanical alloying, J. Alloys Compd. **350**, 296-302 (2003). DOI: https://doi.org/10.1016/S0925-8388(02)00964-7

[6] K. Biswas, J. He, I. Blum, et al., High-performance bulk thermoelectrics with all-scale hierarchical architectures, Nature **489**, 414-418 (2012). DOI: https://doi.org/10.1038/nature11439

[7] A. Michalski, M. Rosiński, Pulse Plasma Sintering and Applications, Adv. Sinter. Sci. Technol. 219-226 (2017).

[8] K.F. Cai, C.W. Nan, X.M. Min, The effect of silicon addition on thermoelectric properties of a B_4C ceramic, Materials Science and Engineering: B **67**, 3, 1999, 102-107 (1999). ISSN 0921-5107. DOI: https://doi.org/10.1016/S0921-5107(99)00220-2

[9] Y. Ohba, T. Shimozaki, H. Era, Thermoelectric Properties of Silicon Carbide Sintered with Addition of Boron Carbide, Carbon, and Alumina, Materials Transactions **49**, 6, 1235-1241 (2008). DOI: http://dx.doi.org/10.2320/matertrans.MRA2007232

[10] M.J. Kruszewski et al., Microstructure and Thermoelectric Properties of Bulk Cobalt Antimonide ($CoSb_3$) Skutterudites Obtained by Pulse Plasma Sintering, J. Electron. Mater. **45**, 1369-1376 (2016). DOI: https://doi.org/10.1007/s11664-015-4037-5

[11] A. Michalski, D. Siemiaszko, Nanocrystalline cemented carbides sintered by the PPS method, Int. J. Refract. Met. Hard Mater. **25**, 153 (2007). DOI: https://doi.org/10.1016/j.ijrmhm.2006.03.007

[12] A.M. Abyzov, M.J. Kruszewski, Ł. Ciupiński, M. Mazurkiewicz, A. Michalski, K.J. Kurzydłowski, Diamond-tungsten based coating-copper composites with high thermal conductivity produced by Pulse Plasma Sintering, Mater. Des. **76**, 97 (2015). DOI: https://doi.org/10.1016/j.matdes.2015.03.056

[13] J. Grzonka, J. Kruszewski, M. Rosiński, Ł. Ciupiński, A. Michalski, K.J. Kurzydłowski, Interfacial microstructure of copper/diamond composites fabricated via a powder metallurgical route, Mater. Charact. **99**, 188 (2015). DOI: https://doi.org/10.1016/j.matchar.2014.11.032

[14] M. Rosiński, J. Wachowicz, T. Płociński, T. Truszkowski, A. Michalski, Properties of WCCO/diamond composites produced by PPS method intended for drill bits for machining of building stones, Ceram. Trans. **243**, 181 (2014). DOI: https://doi.org/10.1002/9781118771464

[15] W. Liu, X. Yan, G. Chen, Z. Ren, Recent advances in thermoelectric nanocomposites, Nano Energy **1**, 42-56 (2012). DOI: https://doi.org/10.1016/j.nanoen.2011.10.001

[16] F. Dąbrowski, Ł. Ciupiński, J. Zdunek, J. Kruszewski, R. Zybała, A. Michalski, K.J. Kurzydłowski, Microstructure and thermoelectric properties of p and n type doped $β-FeSi_2$ fabricated by mechanical alloying and pulse plasma sintering, Materials Today: Proceedings **8**, 2, 531-539 (2019). DOI: https://doi.org/10.1016/j.matpr.2019.02.050

[17] M. Ito, H. Nagai, S. Katsuyama, K. Majima, Thermoelectric properties of $β-FeSi_2$ with B_4C and BN dispersion by mechanical alloying, J. Mat. Science **37**, 2609-2614 (2002). DOI: https://doi.org/10.1023/A:1015891811725

[18] M. Ito, H. Nagai, T. Tanaka, S. Katsuyama, K. Majima, Thermoelectric performance of n-type and p-type $β-FeSi_2$ prepared by pres-sureless sintering with Cu addition, J. Alloys Compd. **319**, 303-311 (2001). DOI: https://doi.org/10.1016/S0925-8388(01)00920-3

[19] N. Niizeki, et al., Effect of Aluminum and Copper Addition to the Thermoelectric Properties of $FeSi_2$ Sintered in the Atmosphere, Mater. Trans. **50**, 1586-1591 (2009). DOI: https://doi.org/10.2320/matertrans.E-M2009808

[20] A. Heinrich, et al., Thermoelectric properties of $β-FeSi_2$ single crystals and polycrystalline $β-FeSi_{2+x}$ thin films, Thin Solid Films **381**, 287-295 (2001). DOI: https://doi.org/10.1016/S0040-6090(00)01758-2

[21] K. Nogi, T. Kita, Rapid production of $β-FeSi_2$ by spark-plasma sintering, J. Mater. Sci. **35**, 5845-5849 (2000). DOI: https://doi.org/10.1023/A:1026752206864

[22] J. Tani, H. Kido, Electrical properties of Co-doped and Ni-doped $β-FeSi_2$, J. Appl. Phys. **84**, 1408 (1998). DOI: https://doi.org/10.1063/1.368174

[23] H. Nagai, M. Ito, S. Katsuyama, K. Majima, The Effect of Co and Ni Doping on the Thermoelectric Properties of Sintered $β-FeSi_2$, Journal of the Japan Society of Powder and Powder Metallurgy, Released December 04, 2009. DOI: https://doi.org/10.2497/jjspm.41.560

[24] H.Y. Chen, X.B. Zhao, C. Stiewe, D. Platzek, E. Mueller, Microstructures and thermoelectric properties of Co-doped iron disilicides prepared by rapid solidification and hot pressing, J. Alloys Compd. **433**, 338-344 (2007). DOI: https://doi.org/10.1016/j.jallcom.2006.06.080

[25] Y. Ohta, S. Miura, Y. Mishima, Thermoelectric semiconductor iron disilicides produced by sintering elemental powders, Intermetallics, **7**, 1203-1210 (1999). DOI: https://doi.org/10.1016/S0966-9795(99)00021-7

[26] H.Y. Chen, X.B. Zhao, T.J. Zhu, Y.F. Lu, H.L. Ni, E. Muller, A. Mrotzek, Influence of nitrogenizing and Al-doping on microstructures and thermoelectric properties of iron disilicide materials, Intermetallics **13**, 704-709 (2005). DOI: https://doi.org/10.1016/j.intermet.2004.12.019

[27] M. Ito, H. Nagai, E. Oda, S. Katsuyama, K. Majima, Effects of P doping on the thermoelectric properties of $β-FeSi_2$, J. Appl. Phys. **91**, 2138-2142 (2002). DOI: https://doi.org/10.1063/1.1436302

[28] X. Qu, S. Lü, J. Hu, Q. Meng, Microstructure and thermoelectric properties of $β-FeSi_2$ ceramics fabricated by hot-pressing and spark plasma sintering, J. Alloys Compd. **509**, 10217-10221 (2011). DOI: https://doi.org/10.1016/j.jallcom.2011.08.070

[29] Y. Ma, R. Heijl, A.E.C. Palmqvist, Composite thermoelectric materials with embedded nanoparticles, J Mater Sci **48**, 2767-2778 (2013). DOI: https://doi.org/10.1007/s10853-012-6976-z

[30] T. Wejrzanowski, Computer Assisted Analysis of Gradient Materials Microstructure, Masters Thesis, Warsaw University of Technology (2000).

[31] K. Nogi, T. Kita, X-Q. Yan, Optimum Sintering and Annealing Conditions for $β-FeSi_2$ Formed by Slip Casting, J. Ceram. Soc. Japan **109**, 265-269 (2001). DOI: https://doi.org/10.2109/jcersj.109.1267_265

[32] G. Shao, K.P. Homewood, On the crystallographic characteristics of ion beam synthesized, Intermetallics **8**, 1405-1412 (2000). DOI: https://doi.org/10.1016/S0966-9795(00)00090-X